A study of the structural changes in Co-Si-B glasses by neutron diffraction

1994 J. Phys.: Condens. Matter 6 1645

(http://iopscience.iop.org/0953-8984/6/9/007)

J. Phys.: Condens. Matter 6 (1994) 1645–1652. Printed in the UK

A study of the structural changes in Co–Si–B glasses by neutron diffraction

L Fernández Barquín†, J C Gómez Sal†, J M Barandiarán‡, F J Bermejo§ and W S Howells¶

† DCITTYM (Materiales) Facultad de Ciencias, Santander 39005, Spain
‡ Departamento Electricidad y Electrónica, UPV Apdo. 644, Bilbao 48080, Spain
§ CSIC-IEM, Serrano 119, Madrid 28006, Spain
¶ ISIS Facility, Rutherford Appleton Laboratory, Chilton, Didcot OX11 0QX, UK

Received 24 June 1993, in final form 21 October 1993

Abstract. Neutron diffraction experiments have been performed to investigate the structure of the ternary $Co_{70}Si_{30-x}B_x$ glasses with $x = 9$, 12 and 21 and $Ni_{70}Si_9B_{21}$ in the 15 to 300 K temperature range. The reduced distribution functions $G(r)$ allow a scrutiny of the contributions of the different pair correlations. The comparison of these functions for compounds with the same Co content has been especially useful in determining the assignments for the first pair distances, which are close to those of the binary alloys.

1. Introduction

The structure of metallic glasses is characterized by the existence of chemical and topological short-range order, giving rise on the whole to an amorphous arrangement. This atomic distribution is not easily described because diffraction methods are often not very conclusive, with a description only of the radial distribution of the atoms. Furthermore, to obtain more detail about correlations between the components of the glassy alloy, it is necessary to perform combinations of different techniques and chemical or isotopic substitutions [1, 2].

During recent years, much effort has been developed successfully in the analysis of the structure of binary alloys, in many cases using neutron diffraction. However, there is much less research into ternary alloys, although these also present a lot of macroscopic properties of interest. The main reason for this lack of study is the great difficulty in extracting structural information about ternary alloys; sometimes, it is even impossible to use the usual substitution methods mentioned above, due to the absence of sufficient isotopes.

The Co-based metallic glasses present magnetic properties suitable for technological applications that have been thoroughly studied [3–5]. Some of the different behaviours observed in these compounds are usually thought of as originating from changes in the short-range-order atomic arrangements (SRO), disregarding the evident lack of direct experimental data to confirm those assumptions [5–7]. Structural investigation of these compounds using neutron diffraction is hard, stemming from the lack of cobalt isotopes and the low scattering length and high absorption of the element. However, in this work, we will try to overcome these drawbacks using samples with the same Co content but with small differences in the metalloid concentration. The comparison of the corresponding diagrams will help the analysis of the different contributions to the reduced distribution functions $G(r)$. In addition, the thermal variation of the $S(Q)$ patterns provides information about the magnetic contributions, as well as the changes in first peak position, which could be related to the low-temperature resistivity behaviour [8].

0953-8984/94/091645+08$19.50

2. Experimental details

The metallic glasses studied are $Co_{70}Si_{21}B_9$, $Co_{70}Si_{18}B_{12}$ and $Co_{70}Si_9B_{21}$. These were chosen because they show outstanding changes in their electrical and magnetic properties (see table 1). Apart from these three compositions, an isomorphous non-magnetic Ni-based compound ($Ni_{70}Si_9B_{21}$) was also studied.

The samples were ribbons about 1 mm wide and 25 microns thick, made by the single-roller quenching method in air (linear speed of disc around 25 m s^{-1}. ^{11}B isotope (92.2% enriched) was used in the castings to avoid the large neutron absorption of natural boron. X-ray analysis was performed on every sample to check whether samples were fully amorphous.

The neutron diffraction experiments were carried out in the wide Q-range LAD diffractometer at ISIS in the Rutherford Appleton Laboratory. The as-cast ribbons (between 3.5 and 6 g) were placed in a thin-walled vanadium container. The temperatures selected for the spectra were 15 K, 80 K, 150 K and room temperature. The spectra have been corrected for background, multiple scattering and attenuation, and normalized using the program package ATLAS [9]. The amorphous character of the samples has also been checked on LAD itself where the detectors at 150° scattering angle have sufficiently good resolution (0.5%), to resolve Bragg peaks. In our patterns, the samples studied did not display any trace of crystallinity. The low-angle detectors (2% resolution) go down to lower values of Q, necessary to calculate the $G(r)$.

3. Results and discussion

The first comment is about the thermal variation of the structure factor. In figure 1, $S(Q)$ is shown at different temperatures for two of the compounds studied. It is obvious that neither the position of the first peak (Q_p), not its intensity show much change. Careful scrutiny of the Q_p positions lead to the values plotted in figure 2, compared with those obtained in a previous experiment [10] at the D1B diffractometer in the ILL. The coincidence of the results from both instruments is remarkable, even though the batches of ribbons used for each of the experiments came from different castings. As was thoroughly documented in a recent article [10], the independence of Q_p with temperature questioned the explanation based on changes in Q_p and $2k_F$ (k_F is the Fermi vector) relative positions (see diffraction model [11]) for the origin of resistivity minima. A resistivity decrease at low temperatures, independent of $S(Q)$ evolution, as proposed by Cote and Meisel [12] for high-resistivity compounds might be more appropriate.

The second comment deals with the magnetic contribution to the $S(Q)$. All the patterns have been collected below T_c; where magnetic scattering exists for Co-based compounds. Nevertheless, as can be seen in figure 1, no noteworthy $S(Q)$ intensity variations are detected, although temperatures reach as much as 0.8 T_c. Indeed, recent high-temperature experiments did not show any special changes (or decay) of the total intensity at T_c [13]. This would mean that the magnetic effects are masked by the large nuclear scattering. In any case, it is evident that a correct estimate of the magnetic scattering would need data from polarized neutron diffraction. To our knowledge, this kind of experiment has never been performed on ternary alloys, only on the binary alloy Co–P [14], Fe–B [15] and Co–B [16], showing a prominent magnetic contribution. It should be noted that T_c in those binary alloys is higher than 550 K, (for example in $Co_{75}B_{25}$, T_c = 788 K); thus, a considerable magnetic contribution is expected. However, for the ternary compounds, T_c are much lower

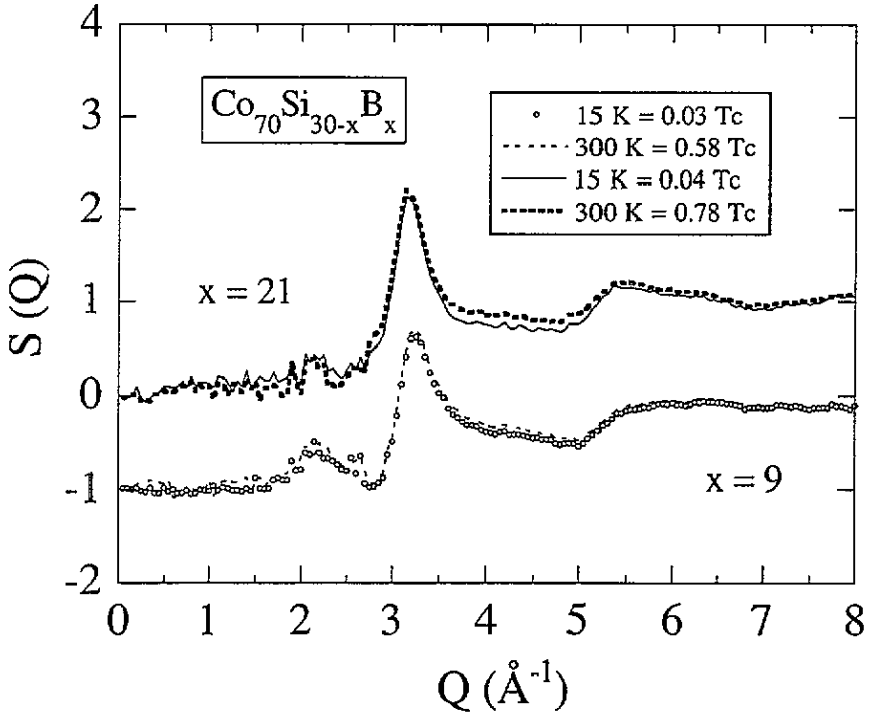

Figure 1. Changes in $S(Q)$ with temperature. The x = 9 spectra have been shifted down to clarify the view.

(see table 1) and very sensitive to metalloid changes, so it is not surprising that magnetic scattering is masked by the nuclear one.

Now, we shall consider the analysis of the reduced distribution functions $G(r)$ in order to obtain information about the structure of these compounds. From the structure factor $S(Q)$, the reduced distribution function is calculated through the expression:

$$G(r) = \frac{2}{\Pi}\int_0^\infty Q[S(Q) - 1]\sin Qr\, dQ. \tag{1}$$

The upper bound of the integral is limited by the experimental Q range, which is Q = 20 Å^{-1} in the present case. This value is similar to those used in other works on metallic glasses [17, 18]. The oscillations in $S(Q)$ are practically damped at higher Q values, especially for Co-based compounds. The $S(Q)$ have been obtained merging high- and low-angle spectra. The inelasticity corrections have been performed using a standard program [9] based on the formulae of Howe *et al* [19].

The reduced $G(r)$ are shown in figures 3 and 4. The counting times for Co samples were about twice those for $Ni_{70}Si_9B_{21}$, however for the latter, $G(r)$ shows more well-defined oscillations and sharper peaks than the Co-based compounds. The reasons for this are the larger incoherent cross section and the higher neutron absorption of cobalt ($\sigma_a(Co) \simeq 8\sigma_a(Ni)$), and also the small ratio between their respective scattering lengths: $(b_{Co}/b_{Ni})^2 = \frac{1}{16}$ [20]. In spite of this difficulty, general trends may be stated for both Ni and Co compounds.

The theoretical expression for the total structure factor, considering partial structure factors is given by the following equation (2) for a ternary ABC compound:

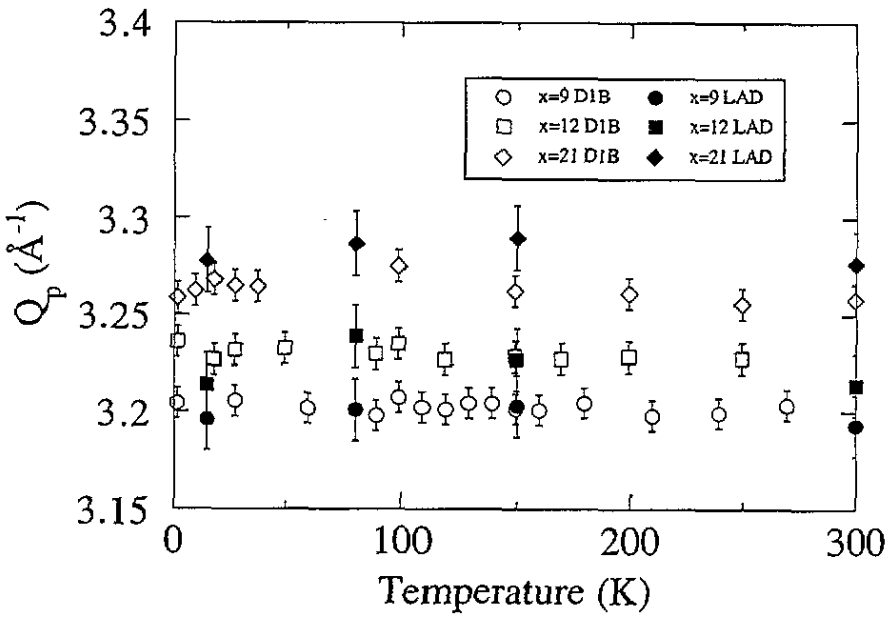

Figure 2. Position of the maximum in $S(Q)$ (Q_p) for the $Co_{70}Si_{30-x}B_x$ compounds. Data from D1B (ILL) plotted as open marks. Data from LAD (ISIS) are full marks.

Table 1. Characteristic parameters of the studied compounds. Numbers of parentheses denote value uncertainty. T_c: Curie temperature; σ_S: saturation magnetization at 4.2 K; T_{min}: temperature of resistivity minimum; ρ: absolute resistivity at 300 K.

Composition	T_c (K)	σ_s (emu g^{-1})	T_{min} (K)	ρ ($\mu\Omega$ cm)
$Co_{70}Si_9B_{21}$	512(1)	79.00(1)	42(1)	118(6)
$Co_{70}Si_{18}B_{12}$	386(1)	66.06(1)	94(1)	137(7)
$Co_{70}Si_{21}B_9$	335(1)	59.44(1)	132(1)	139(7)
$Ni_{70}Si_9B_{21}$	—	—	24(1)	142(7)

$$S(Q) = \frac{1}{\langle b\rangle^2}\left(\sum_i c_i^2 b_i^2 S_{ii}(Q) + \sum_{i\neq j} c_i c_j b_i b_j S_{ij}(Q)\right) \qquad i, j = \text{A, B, C} \tag{2}$$

where c_i are the concentrations, b_i their respective scattering lengths and $\langle b\rangle = c_A b_A + c_B b_B + c_C b_C$.

As commented above, we have to work with total $S(Q)$ functions as it is impossible to extract partial distributions with any of the usual procedures. A way to proceed with the analysis is to compare the measured $G(r)$ with the data from partial correlation functions in binary alloys. Table 2 shows the interatomic pair distances of binary glasses collected from the literature.

3.1. $Ni_{70}Si_9B_{21}$

In this case, the equation (2) becomes:

$$S(Q) = 0.644S_{\text{Ni-Ni}}(Q) + 0.25S_{Ni-B}(Q) + 0.066S_{\text{Ni-Si}}(Q) + 0.024S_{\text{B-B}}(Q) + 0.013S_{\text{Si-B}}(Q) + 0.002S_{\text{Si-Si}}(Q). \tag{3}$$

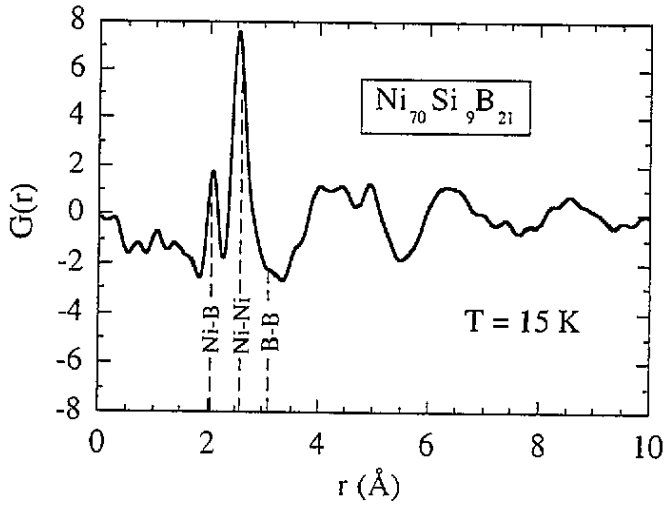

Figure 3. Reduced distribution function $G(r)$ of $Ni_{70}Si_9B_{21}$ at T = 15 K. The vertical dashed lines indicate pair distances from table 2.

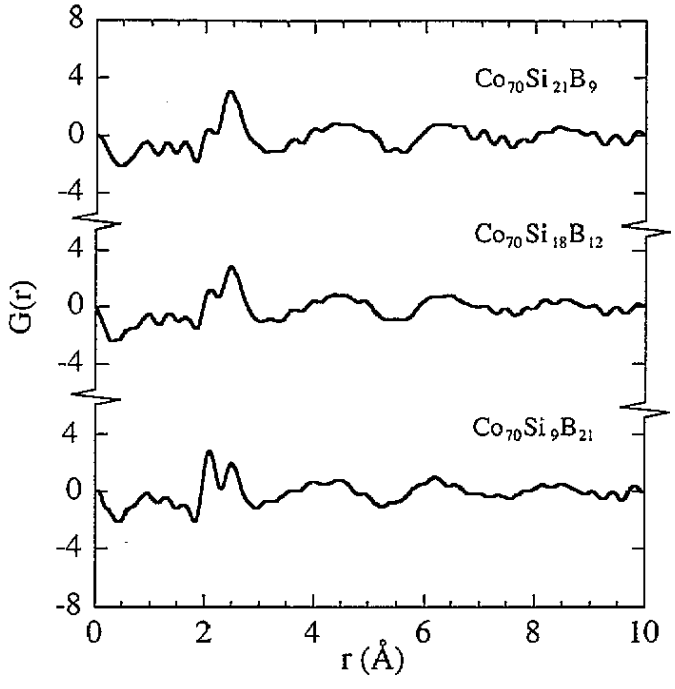

Figure 4. Reduced distribution functions $G(r)$ of the studied Co-based compounds at T = 15 K.

So, the largest contribution stems from Ni–Ni and Ni–B pairs. In figure 3 we indicate with vertical lines the distances from table 2. Two well-defined peaks appear between 2 Å and 3 Å in a rather good coincidence with the Ni–B and Ni–Ni lines, respectively. Thus, this assignment seems convenient. There are no data in table 2 available for the Ni–Si pair

Table 2. Interatomic pair distances (M–M, M–m and m–m; M = metal, m = metalloid) for binary alloys reported in previous works.

Pair	Distance 1 (Å)	Distance 2 (Å)	Material[Ref.]
Fe–Fe	2.60	4.20	$Fe_{75}B_{25}$ [18]
Fe–B	2.18	3.85	"
Fe–Fe	2.57	4.20	$Fe_{80}B_{20}$ [25]
Fe–B	2.14	3.79	"
B–B	3.57	—	"
Co–Co	2.57	—	$Co_{78}B_{22}$ [16]
Co–Co	2.57	—	$Co_{74}B_{26}$ [16]
Co–Co	2.6	—	$Co_{80}B_{20}$ [24]
Co–B	2.1	—	"
Ni–Ni	2.5	4.2	$Ni_{81}B_{19}$ [21]
Ni–B	2.1	3.8	"
B–B	3.2	3.9	"

distances. Furthermore due to the small Ni–Si contribution to the total $S(Q)$, it is presumed that it cannot be detected separately in the pattern. The larger size of Si atoms makes it probable that this contribution lies in the second peak. (This hypothesis will be corroborated in the discussion of Co-based compounds.) The smaller values of the coefficients for Si–Si and B–B explain the absence of such peaks which could be expected for $r > 3.0$ Å (see table 2).

At longer distances, $r > 3.5$ Å, the typical subtle split in metallic glasses appears, but it seems reasonable to avoid any peak identification. However, the pattern is quite different to those obtained for binary alloys (see figure 3, table 2 and [21]), suggesting different long-distance arrangement for the ternary alloys.

3.2. Co-based compounds

In the same way, the general formula (2) gives:

(i) $Co_{70}Si_9B_{21}$:

$$S(Q) = 0.395S_{Co-B}(Q) + 0.25S_{Co-Co}(Q) + 0.156S_{B-B}(Q) + 0.105S_{Co-Si}(Q) + 0.083S_{Si-B}(Q) + 0.011S_{Si-Si}(Q). \quad (4)$$

(ii) $Co_{70}Si_{18}B_{12}$:

$$S(Q) = 0.285S_{Co-Co}(Q) + 0.258S_{Co-B}(Q) + 0.24S_{Co-Si}(Q) + 0.108S_{Si-B}(Q) + 0.058S_{B-B}(Q) + 0.051S_{Si-Si}(Q). \quad (5)$$

(iii) $Co_{70}Si_{21}B_9$:

$$S(Q) = 0.299S_{Co-Co}(Q) + 0.293S_{Co-Si}(Q) + 0.202S_{Co-B}(Q) + 0.099S_{Si-B}(Q) + 0.072S_{Si-Si}(Q) + 0.034S_{B-B}(Q). \quad (6)$$

Figure 5 shows the $G(r)$ for the three Co–Si–B compounds. The poorer statistics of cobalt compounds compared to the Ni one makes more ripples appear at $r < 1.8$ Å and also reduces the intensity of the main peaks, which again appear at 1.8 Å $< r <$ 3.2 Å. Following the discussion for Ni–Si–B compound, the first of these peaks could correspond to the Co–B pair and the second (around 2.5 Å) to Co–Co pair. This latter shifts to higher distances when the B content increases. The Co–Si contribution is supposed to lie in the

second peak. This assessment can be confirmed by looking at the variation with composition of the intensity of $G(r)$ peaks. In fact, it is clearly seen that the first peak (Co–B) increases when the boron concentration is increased, while the second peak (Co–Co and Co–Si) increases with increasing silicon content, certainly due to the Co–Si pair contribution. This confirms that M–Si (M = Ni, Co) effectively lies in this peak. The Ni–Si contribution was negligible but this is not the case for Co-based compounds, leading to notable changes in the intensities of $G(r)$ peaks when changing the Si content.

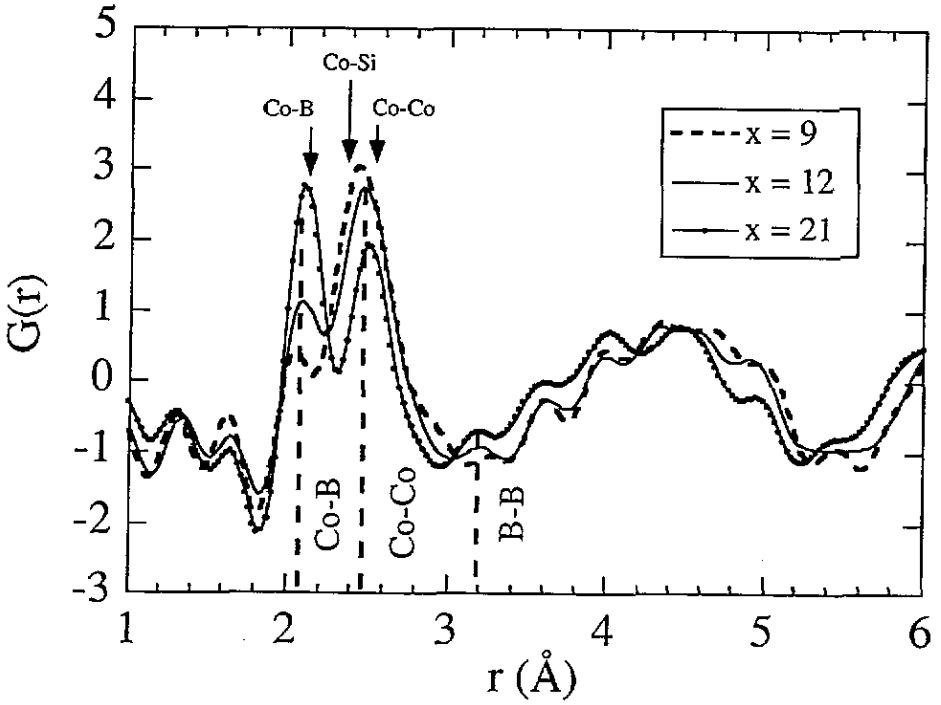

Figure 5. Larger scale $G(r)$ for $Co_{70}Si_{30-x}B_x$ at T = 15 K. The dashed vertical lines show the pair positions from table 2. Arrows mark positions obtained from this study.

For the long-distance region, we can just point out, like for $Ni_{70}Si_9B_{21}$, that these compounds differ in their atomic ordering with respect to those of binary alloys.

Besides estimating the pair distances, it is possible to calculate the coordination numbers Z of first neighbours through the radial distribution function (RDF) (the densities have been deduced from the formula in [22]). As commented above, the contribution of the Ni–Si pair is negligible. So, the main contribution to the second peak is the Ni–Ni pair, thus making satisfactory fits of the two main peaks to a pair of Gaussian functions. The coordination numbers for the nearest distances (Z_{Ni-B} = 1.9±0.2, Z_{B-Ni} = 6.3±0.8 and Z_{Ni-Ni} = 8.3±0.8) are slightly lower than those of the binary alloys [18], being these differences due to the presence of Si atoms.

On the other hand, this analysis for Co-based compounds is extremely difficult because there are three main contributions (Co–B, Co–Co and Co–Si) of low intensity. Attempts have been made to fit the first two peaks to three Gaussians: one centred at the first peak and the other two in the second one (see the clear asymmetry of this second peak in figure 5). Although the coordination numbers could not be calculated with enough accuracy,

the estimated distances for Co–Co and Co–B are very close to those in table 2, and the Co–Si distance (for example in $Co_{70}Si_{18}B_{12}$, r_{Co-Si} = 2.38 Å) has similar values to that of EXAFS data, which is the addition of the covalent radii of Co and Si [23].

To conclude, the reduced distribution functions $G(r)$ in these ternary compounds can be extracted from the $S(Q)$, resulting in two well-defined peaks at distances up to 3.3 Å, and displaying short-range arrangements near to those of binary alloys. For longer distances, the atomic arrangements also look different. Choosing compounds with fixed metal quantity but varying the metalloid concentration allows peak assignments thanks to the relative variations of the intensities of the peaks. This is interesting for ternary alloys where it is not feasible to extract partial functions by the usual procedure of isotopic and chemical substitutions and comparison with x-ray diffraction.

Acknowledgments

This work has been supported by CICYT, (grant MAT-90-0877).

References

[1] Elliot S R 1983 *Physics of Amorphous Materials* (Harlow: Longman Scientific & Technical) p 316
[2] Sadoc J F and Wagner C N J 1983 *Glassy Metals II* ed H Beck and H Güntherodt (Berlin: Springer) p 51
[3] Maszkiewicz M 1982 *J. Appl. Phys.* **53** 7765
[4] Kulik T, Matyja H and Lisowski B 1984 *J. Magn. Magn. Mater.* **43** 135
[5] Vázquez M, Ascasibar E, Hernando A and Nielsen O V 1987 *J. Magn. Magn. Mater.* **66** 37
[6] Maszkiewicz M, Zochowski S, Cumming A and Fawcett E 1987 *J. Magn. Magn. Mater.* **67** 193
[7] Fernández Barquín L, Rodríguez Fernández J, Gómez Sal J C, Barandiarán J M and Vázquez M 1990 *J. Appl. Phys.* **68** 4610
[8] Mizutani U 1983 *Prog. Mater. Sci.* **28** 97
[9] Soper A K, Howells W S and Hannon A C 1989 *RAL Report* 89-046
[10] Fernández Barquín L, Rodríguez Fernández J, Gómez Sal J C, Gutiérrez J and Barandiarán J M 1991 *J. Magn. Magn. Mater.* **101** 52
[11] Nagel S R 1977 *Phys. Rev.* B **16** 1694
[12] Cote P J and Meisel L V 1981 *Glassy Metals I* ed H Beck and H Güntherodt (Berlin: Springer) p 150
[13] Fernández Barquín L, Vázquez M, Barandiarán J M and Rodríguez Carvajal J 1991 *Spanish Research using Neutron Scattering Techniques* ed J C Gómez Sal, F Rodríguez, J M Barandiarán, F Plazaola and T Rojo (Universidad de Cantabria) p 148
[14] Bletry J 1979 *Thesis* Grenoble University
[15] Guoan W, Cowlam N, Davies H A, Cowley R A, McK Paul D and Stirling W G 1982 *J. Physique* **43** C7–71
[16] Dubois J M, Le Caer G, Chieux P and Goulon J 1982 *Nucl Instrum. Methods* **199** 315
[17] Sváb E, Kroó N, Ishmaev S N, Shadikov I P and Chernyshov A A 1983 *Solid State Commun.* **46** 351
[18] Matz W, Hermann H and Mattern N 1987 *J. Non-Cryst. Solids* **93** 217
[19] Howe M A, McGreevy R L and Howells W S 1989 *J. Phys.: Condens. Matter* **1** 3433
[20] Lovesey S W 1984 *Theory of Neutron Scattering from Condensed Matter* (Oxford: Clarendon) vol I, p 1
[21] Lamparter P, Sperl W, Nold E, Rainer-Harbach G and Steeb S 1982 *Rapidly Quenched Metals IV* ed T Masumoto and K Suzuki (Sendai: Japan Institute of Metals) p 343
[22] Aso K, Hayakawa M, Hotai K, Uedaira S, Ochiai Y and Makino Y 1982 *Rapidly Quenched Metals IV* ed T Masumoto and K Suzuki (Sendai: Japan Institute of Metals) p 379
[23] Fdez-Gubieda M L, Barandiarán J M, Plazaola F, Hernando A and Mobilio S 1992 *J. Non-Cryst. Solids* **151** 51 and references therein
[24] Davidovic M, Howells W S and Rhyne J J unpublished
[25] Nold E, Lamparter P, Olbrich H, Rainer-Harbach G and Steeb S 1981 *Z. Naturforsch* **36A** 1032